

A folded Fabry-Perot diplexer of triangular shape.

Herman van de Stadt

Space Research Organization Netherlands,
SRON, PO box 800, 9700 AV Groningen, The Netherlands.

fax +31 503634033, h.vandestadt@sron.rug.nl

10th Space THz Symposium, Charlottesville, March 16-18, 1999.

ABSTRACT.

In this paper we present a novel triangular, multiple-beam diplexer. Its properties are compared with existing square diplexers. Our triangular folded Fabry-Perot (FFP) diplexer is a ring-interferometer consisting of two partially-transparent mesh filters and a slightly concave mirror. The reflector is tunable in position and the three components are mounted in the shape of a triangle with 60-degree angles. The purpose of the diplexer is to superimpose a signal and a local oscillator (LO) beam with frequencies of order 1 THz and a difference frequency of order 10 GHz.

INTRODUCTION.

The operation of a THz heterodyne receiver in space requires a large IF bandwidth in order to increase the speed of line surveys and to allow observation of broad weak line emission from distant galaxies. For example the HIFI instrument on board of FIRST will have a 4 GHz IF bandwidth for RF frequencies ranging from 480 GHz to over 2.5 THz [1].

For efficient coupling of the signal and the local oscillator (LO) power to the mixer one often uses diplexers to combine the signal and LO beams. A diplexer is an interferometer allowing nearly loss-less superposition of two beams of different frequency. The optical path length in the interferometer, L_{opt} , is related to the difference, or intermediate frequency IF by:

$$L_{opt} = c / (2 IF) \quad (1)$$

The usual diplexer in heterodyne receivers is a dual-beam, polarizing Martin-Puplett [2] interferometer, (MP). However, its transmission is sinusoidal as a function of frequency, which makes this interferometer less suitable for wide IF bandwidths. Wide

bandwidths have been achieved with multiple-beam interferometers of the Fabry-Perot type in a folded version, originally proposed by Gustinic [3]. General properties of the mentioned interferometers are described in ref [4].

In table I we give the calculated efficiency (i.e. transmission) of a loss-less MP diplexer in the case of a 6 and a 10 GHz IF center frequency and 4 GHz bandwidth. Also given is the efficiency (i.e. reflection) of a loss-less FFP diplexer for the same IF frequencies and for mirror reflectivities of 67% and 77%, i.e. a finesse of 7.8 and 12.0, respectively .

| Diplexer type | Efficiency @ IF center frequency | Efficiency @ IF center freq. \pm 2 GHz |
|---------------------------------|----------------------------------|--|
| Martin-Puplett @ IF= 6 GHz | 1.0 | 0.75 |
| Idem @ IF=10 GHz | 1.0 | 0.90 |
| Fabry-Perot, R=0.67 @ IF= 6 GHz | 0.961 | 0.949 |
| Idem, @ IF=10 GHz | 0.961 | 0.957 |
| Fabry-Perot, R=0.77 @ IF= 6 GHz | 0.983 | 0.978 |
| Idem, @ IF=10 GHz | 0.983 | 0.981 |

Table I: Calculated efficiency of loss-less diplexers with 4 GHz bandwidth.

In practice diplexers are never loss-less. Some sources of loss can be:

- coupling losses because of small diplexer size as compared to QO beam size,
- scattering or absorption losses at wire grids or mesh filters,
- coupling losses due to imperfect re-imaging of multiple beams,
- imperfect angular alignment of diplexers' optical components.

Design aspects of our triangular diplexer will be discussed in this paper against the background of the mentioned loss mechanisms. Some measurements illustrate its performance.

DESIGN AND QUASI-OPTICAL PROPERTIES .

Figure 1 gives a schematic diagram of the triangular FFP. The signal beam is reflected upon incidence on the first mesh filter, while the LO is transmitted by the FFP after incidence on the other mesh. Note that the reflector and the meshes have a width W and that the roundtrip path of the multiple reflected beams is:

$$L_{opt} = 3 W / 2 \tag{2}$$

The curvature of the reflector is such that it re-images the minimum beam waist, w_0 , of the quasi-optical beams at a distance z_f from the center of the mirror, where

$$z_f = 3 W / 4 \tag{3}$$

Note however that this does not mean that the focal distance of the mirror is z_f , except in the case that the FFP is used in the far-field region of the propagating beams. We will come back to this later on.

Figure 2 is a graph of the calculated reflection of LO and signal beams for an FFP with $R=0.67$. The figure illustrates the case that ΔIF is $2/3$ of the center IF frequency, representing a bandwidth of one octave.

Propagation of a wavefront with beam radius $w(z)$ at distance z from the (minimum) waist w_0 goes as:

$$w(z)^2 = w_0^2 (1 + z^2/z_R^2) \quad (4)$$

, where $z_R = \pi w_0^2 / \lambda$ is the confocal or Rayleigh distance, see ref [4], eq. (2.21b), and w_0 is the beam waist radius. If we require that the mirror must have a projected size sufficiently large for 4 beam radii, we have approximately:

$$W = 4 w(z_f) \sqrt{3} \quad (5)$$

Combination of eqs. (5) and (4) with $z = z_f$ (3) gives:

$$(w_0)^4 - 3 W^2 (w_0)^2 / 64 + 9 W^2 \lambda^2 / (16 \pi)^2 = 0 \quad (6)$$

Solving this equation for w_0 gives the two values of w_0 for the extreme cases of near- and the far-field. The minimum value of the expression yields the size of w_0 for the case of confocal imaging.

As an example we take $IF = 6$ GHz and $f = 800$ GHz, i.e. $\lambda = 0.375$ mm. This yields $L_{opt} = 25$ mm, $W = 16.67$ mm and $z_f = 12.5$ mm. In table II we summarize the values for w_0 and $w(z_f)$ for the near-field, confocal field and the far-field. This is further illustrated in figure 3, where the propagating beam waists at $+w$ and $-w$ are drawn.

| | w_0 (mm) | $w(z_f)$ (mm) | z_R (mm) |
|------------|------------|---------------|------------|
| Near-field | 3.58 | 3.61 | 107.6 |
| Confocal | 1.22 | 1.73 | 12.5 |
| Far-field | 0.42 | 3.61 | 1.45 |

Table II: Quasi-optical parameters of a triangular FFP with $IF = 6$ GHz and $f = 800$ GHz.

From table II and figure 3 it can be seen that in the confocal case the beam does not use the corners of the diplexer and allows ample space for mechanical support of the mesh filters. In the near-field and far-field however there is no space for mechanical support, making these extreme cases not realistic for beam diameters of 4 waists. In other words the efficiency of the diplexer will be reduced by truncation of the beams.

The question is whether there will always be a confocal situation possible. The answer is that this depends on frequency: there will be a lowest frequency where 4 beam waists are just transmitted by the diplexer. The minimum frequency is determined by calculating the value of λ for which eq. (6) has a single root. This gives:

$$f_{\min} = 96 \text{ IF} / \pi \quad (7)$$

For $\text{IF} = 6 \text{ GHz}$ we find 183 GHz as the minimum frequency of a triangular diplexer. This is much lower than the value of 489 GHz , which we find for an equivalent square diplexer.

MIRROR CURVATURE.

The radius of curvature, $R(z)$, of a Gaussian beam propagating along the z axis is described by the following equation:

$$R(z) = z (1 + z_R^2 / z^2) \quad (8)$$

, where z_R is the confocal distance as before. The mirror of the diplexer should have an elliptical shape in order to match the Gaussian beam wavefront, see ref [5]. For a triangular diplexer the angle of incidence is 30° , which means that the semi-major axis of the ellipse is $a = R_f = R(z_f)$, where R_f is the radius of curvature of the wavefront when it hits the mirror. This is further illustrated in figure 4. Note that R_f is always larger than z_f , except in the far-field, where R_f is approaching z_f because $z \gg z_R$. The effective radii of curvature of the elliptical mirror in the horizontal and vertical direction are:

$$R_{\text{hor}} = 2 R_f / \sqrt{3} \quad \text{and} \quad R_{\text{vert}} = R_f \sqrt{3} / 2 \quad (9)$$

For example in the earlier case with $\text{IF} = 6 \text{ GHz}$ and $f = 800 \text{ GHz}$ we find the following values:

| | Confocal distance, z_R (mm) | Wavefront radius of curvature, R_f (mm) | Horizontal radius of ellipse, R_{hor} (mm) | Vertical radius of ellipse, R_{vert} (mm) |
|------------|-------------------------------|---|---|--|
| Near-field | 107.6 | 939.3 | 1085 | 813 |
| Confocal | 12.5 | 25 | 28.88 | 21.65 |
| Far-field | 1.45 | 12.67 | 14.63 | 10.97 |

Table III: Properties of the elliptical mirror in a triangular diplexer for $\text{IF} = 6 \text{ GHz}$ and $f = 800 \text{ GHz}$.

POLARIZATION.

The resonant frequencies in a triangular diplexer are polarization dependent because of the odd number of reflections. This is not a problem in general, since the LO and signal beams need to have identical polarizations (linear in horizontal or vertical direction) anyway. For the LO beam it means that the cross-polarized component of the beam is not transmitted by the triangular diplexer.

BEAM SYMMETRY.

Off-axis beams propagate through the triangular FFP in an asymmetric way. This is illustrated in figure 5, which gives the trajectories for the central beam and one off-axis beam. After multiple reflections inside the interferometer the off-axis beam propagates alternately above and below the central beam. For symmetric beam modes this is not a problem, since the round-trip optical path is independent on the amount of offset. However, asymmetric modes with 180° phase difference between the upper and lower halves of their mode pattern will be attenuated by this phenomenon.

COMPARISON BETWEEN TRIANGULAR AND SQUARE FFPs.

In the preceding sections we have derived equations for triangular FFPs. Similar equations have been derived for square FFPs (ref [5]) and can be derived for modified versions of triangular FFPs.

In table IV, at the end of this paper, we give parameters of four different FFPs:

1. a square FFP with a single curved mirror,
2. the same as 1, but with 2 curved mirrors,
3. the triangular FFP as described in this paper,
4. a diamond FFP with 60° top angle.

Relevant parameters have been mentioned in the preceding chapters. To quantify the various parameters in the table we calculated the values for the case $f=6$ GHz and $f=800$ GHz, which may be applicable to the HIFI instrument of FIRST.

In order to get a feel of the optical aperture of the beams we added to the table the so-called F-ratio. This parameter, F/D , corresponds to an 11 dB edge taper, i.e. we assumed an "optical diameter", D , for which the beam waist radius in the far field is $w = 0.889 D/2$. This applies e.g. to the quasi-optical beam at the secondary mirror of the FIRST telescope.

From table IV we can see that the triangular FFP has the lowest f_{min} and consequently the widest range of possible F/D ratios. The diamond shaped FFP can be regarded as a deformed square FFP with the advantage that the focal distance, z_f , of the mirrors is more than 4 times larger. This means that the mirror in the diamond FFP will

be much less strongly curved than in the square case. Moreover, the resonances of the diamond FFP are independent of polarization, in contrast to the triangle FFP.

The square FFP with a single curved mirror offers a minimum of flexibility for the chosen frequency: in its confocal case we have $w_0 = 1.22$ mm, which means that 4 beam radii at the mirror ($4 w_0 \sqrt{2} = 6.9$ mm) is larger than the projected mirror size ($W \sqrt{2} = 5.72$ mm). This is equivalent to saying that only 3.6 beam radii fit instead of the desired 4 beam radii.

ALTERNATIVE CONFIGURATIONS.

Many alternative configurations of FFPs can be thought of. However, it is not possible to combine any set of FFPs like with a box of bricks, because the images of multiple beams must be coinciding.

We want to mention one version consisting of two triangles in series: see figure 6. Effectively this is a 3-mirror FFP, discussed in the literature [6] and actually tested at 490 GHz [7, 8]. One advantage of this configuration is that the transmission peak for the LO becomes wider without reducing the reflection of the signal. Thus the required tuning accuracy is reduced. Another advantage is that the two outer reflectors can have a much-reduced reflectivity, $R_1 = R_3 = 0.243$, so that presumably scattering and/or absorption losses in the 2 outer grids will be reduced. Moreover, the asymmetry for off-axis beams, as was illustrated in figure 5 for a single triangular FFP, is now removed.

However, disadvantages of the setup of figure 5 are as follows. The 2 triangles need to have identical optical pathlengths and the tuning mechanism must maintain this equality. Also, in this design the difference in resonances between the two linear polarizations still exists.

EXPERIMENTAL RESULTS.

The use of a square FFP was recently reported [9] at IF = 6 GHz and $f=640$ GHz. Another application of square FFPs can be found in ref [10], describing the heterodyne instrument in UARS-MLS, where an FFP is used for frequencies of 205 and 268 GHz.

At SRON we have built a prototype triangular FFP using 2 inductive, nickel mesh filters of 150 lines/inch providing a reflectivity of about 73% and a plane reference reflector. The measured reflection and transmission as a function of mirror position are given in figure 7 for a frequency of about 345 GHz.

The magnitude of scattering and absorption losses in mesh filters are not well known, but will certainly be present. In this respect further tests on triangular FFPs need to be performed in the future.

CONCLUSIONS.

THz heterodyne receivers in space require the use of diplexers in order to efficiently couple the available LO power to the mixer. Application of a folded Fabry-Perot (FFP) diplexer is especially useful in heterodyne receivers requiring a wide IF bandwidth for a relatively low IF center frequency.

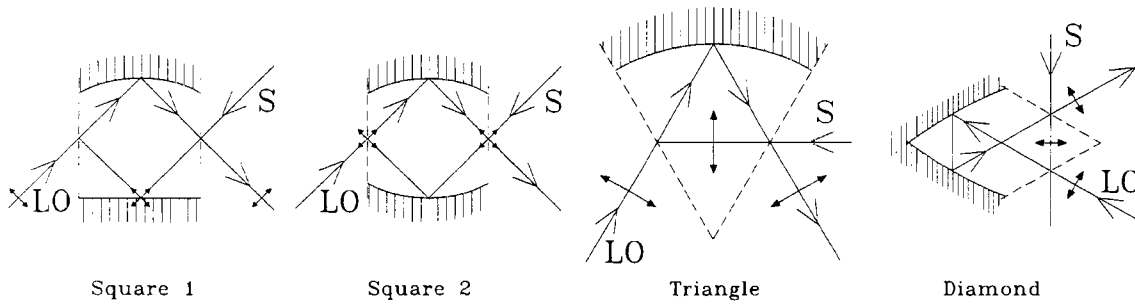
In this paper we described the properties of an FFP with triangular cross-section. The main advantage over the usual FFP with square cross-section is the larger size of the triangle, allowing accommodation of a much wider range of different beam sizes. We have demonstrated the feasibility with a prototype triangular FFP.

ACKNOWLEDGEMENTS.

The author wants to thank Th. de Graauw, N. Whyborn and P. Zimmermann for stimulating this research and D. Beintema for carefully reading the manuscript.

REFERENCES.

- [1] N.D. Whyborn, "The HIFI heterodyne instrument for FIRST: Capabilities and Performance", Proc. of ESA symp The Far Infrared and Submillimetre Universe, Grenoble, ESA SP-401, p.19-24, Aug 1997.
- [2] D.H. Martin and E. Pulett, "Polarised Interferometric Spectroscopy for the Millimetre and Sub-millimetre Spectrum", *Infrared Phys.*, 10, 105 (1969).
- [3] J.J. Gustincic, "A quasi-optical receiver design", *IEEE-MTT-S Int. Microwave Symp. Dig.*, 99-101, 1977.
- [4] P.F. Goldsmith, "Quasi-Optical Systems", IEEE press, ISBN 0-7803-3439-6, 1998.
- [5] H.M. Pickett and A.E.T. Chiou, "Folded Fabry-Perot Quasi-Optical Ring Resonator Diplexer: Theory and Experiment," *IEEE Trans. Microwave Theory Tech.* **MTT-31**, 373 (1983).
- [6] M.M. Pradhan, "Multigrad Interference Filters for the Far Infrared Region", *Infr. Phys.*, Vol. 11, 241-245, 1971.
- [7] H. van de Stadt and J.M. Muller, "Multimirror Fabry-Perot interferometers", *JOSA*, **A2**, 1363-1370, 1985.
- [8] S.J. Hogeveen and H. van de Stadt, "Fabry-Perot interferometers with three mirrors", *Appl. Opt.*, 25, 4181-4184, 1986.
- [9] P.H. Siegel et al. , "A 640 GHz Planar-Diode Fundamental Mixer/Receiver", preprint, June 1998.
- [10] "Eos MLS Instrument Conceptual Design", ESA conference report, Appendix B-1, 1997.



| | Square 1 | Square 2 | Triangle | Diamond |
|--|---------------------------|-----------------|-------------------|-------------------|
| Size W | $W1 = c / (4\sqrt{2} IF)$ | $W2 = W1$ | $W3 = c / (3 IF)$ | $W4 = c / (6 IF)$ |
| Optical Path L_{opt} | $2 W1 \sqrt{2}$ | $2 W2 \sqrt{2}$ | $3 W3 / 2$ | $3 W4$ |
| Focal distance z_f | $W1 \sqrt{2}$ | $W2 / \sqrt{2}$ | $3 W3 / 4$ | $5 W4 / 4$ |
| Minimum freq. f_{min} | $512 IF / \pi$ | $256 IF / \pi$ | $96 IF / \pi$ | $320 IF / \pi$ |
| Values for $IF=6$ GHz and $f = 800$ GHz | | | | |
| W | 8.84 mm | 8.84 mm | 16.67 mm | 8.33 mm |
| Zf | 4.42 mm | 2.21 mm | 12.50 mm | 10.41 mm |
| f_{min} | 978 GHz | 489 GHz | 184 GHz | 612 GHz |
| wO for Near field | - | 1.48 mm | 3.58 mm | 1.64 mm |
| wO for Confocal | (1.22 mm) * | 0.86 mm | 1.22 mm | 1.12 mm |
| wO for Far field | - | 0.51 mm | 0.42 mm | 0.76 mm |
| F/D for beam with 11 dB edge taper. | | | | |
| F/D for Near field | - | 5.51 | 13.35 | 6.09 |
| F/D for Confocal | - | 3.22 | 4.55 | 4.15 |
| F/D for Far field | - | 1.88 | 1.55 | 2.83 |

Table IV: Summary of properties of different types of folded Fabry-Perot diplexers. The *symbol indicates that the design frequency is lower than the minimum frequency.

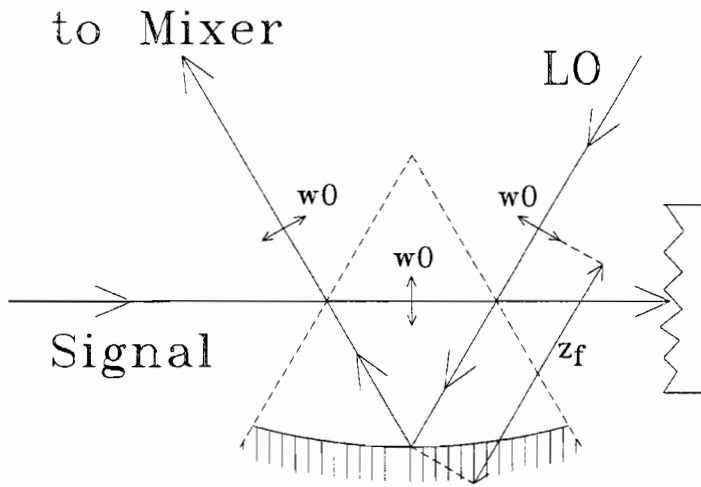


Figure 1: Schematic diagram of a triangular FFP.

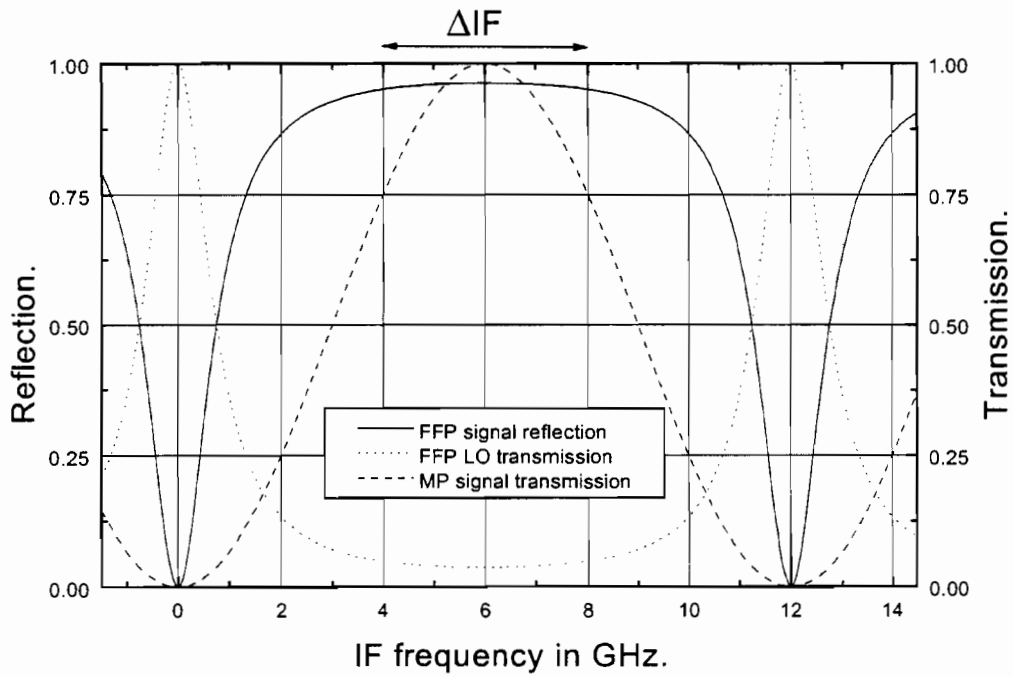


Figure 2: Calculated reflection of the signal beam and transmission of LO beam in a FFP with $R = 0.67$. For comparison we also give the transmission of a Martin Puplett interferometer.

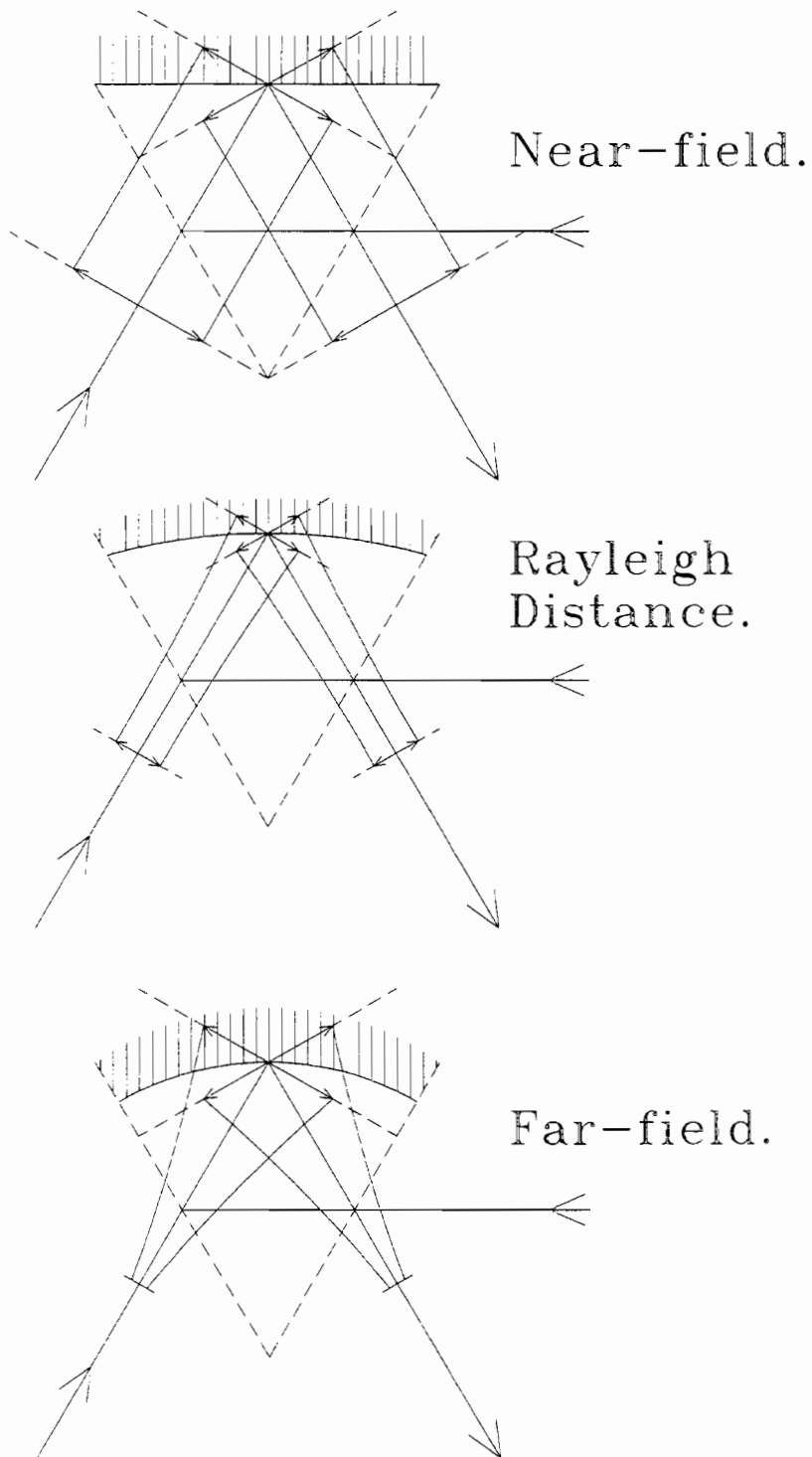
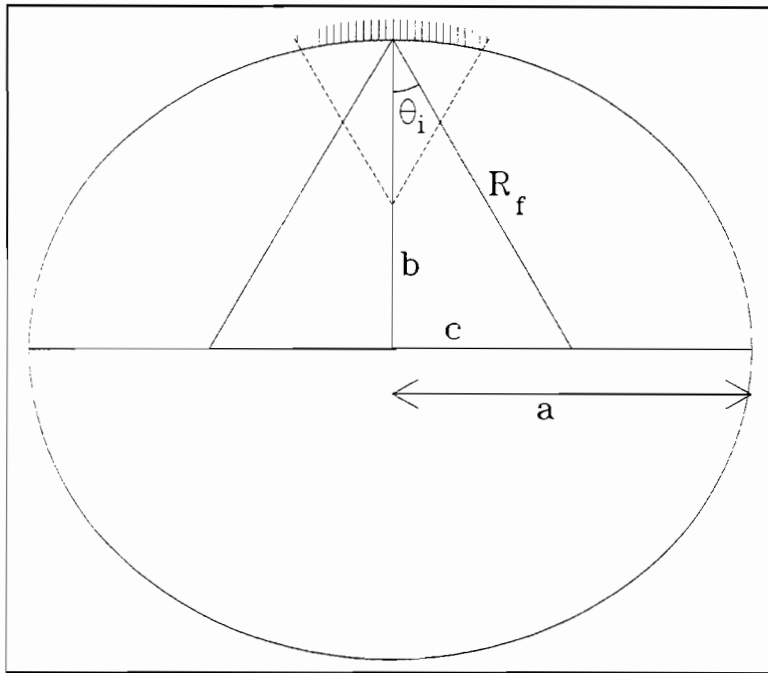


Figure 3: Quasi-optical beam trajectories in a triangular FFP for IF = 6 GHz and $f = 800$ GHz. The pictures are an illustration of the values in Table II.

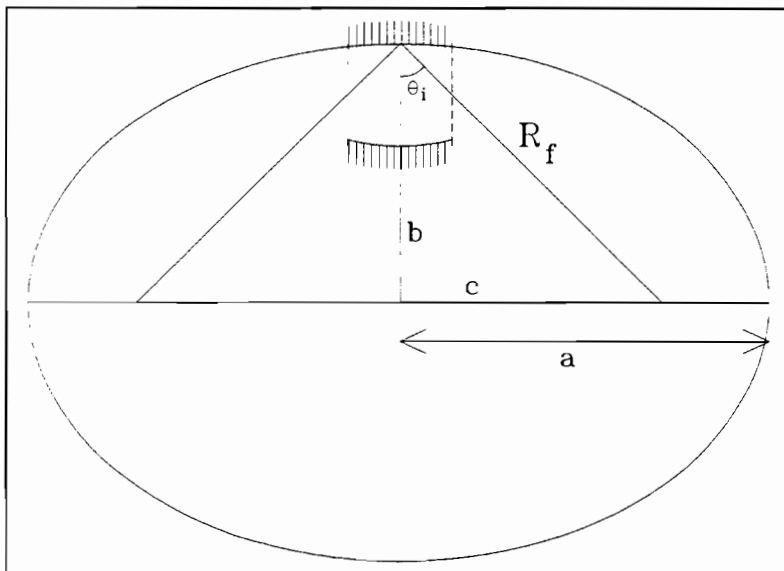


$$\theta_i = 30^\circ$$

$$a = R_f = 2c \quad \epsilon = 0.5$$

$$c = a/2 \quad b = a\sqrt{3}/2$$

Figure 4a: Geometry of the elliptical reflector in a triangular FFP with $\theta_i = 30^\circ$.



$$\theta_i = 45^\circ$$

$$a = R_f = c\sqrt{2} \quad \epsilon = 1/\sqrt{2}$$

$$c = b = a/\sqrt{2}$$

Figure 4b: Geometry of the elliptical reflector in a square FFP with $\theta_i = 45^\circ$.

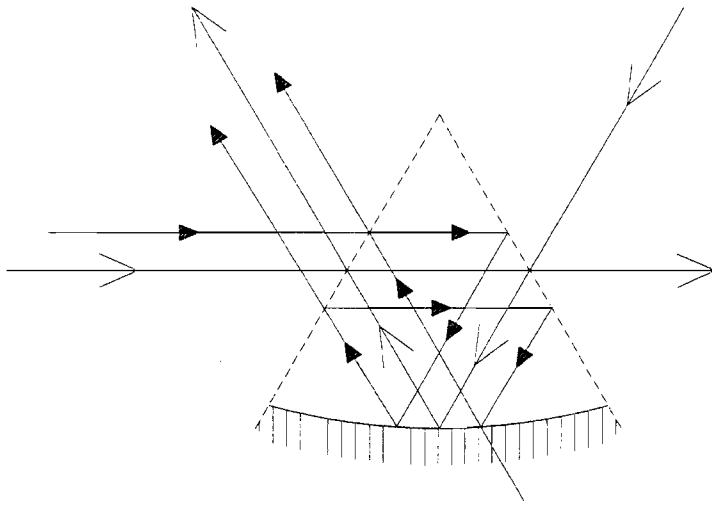


Figure 5: Trajectories of off-axis beams in a triangular FFP.

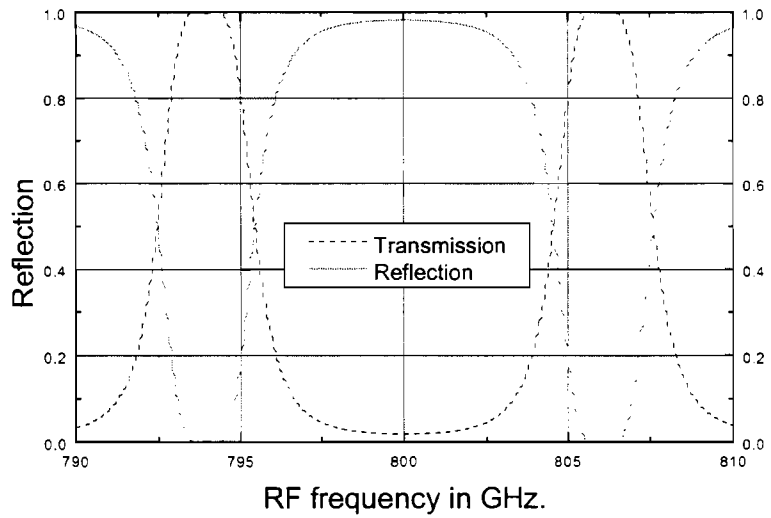
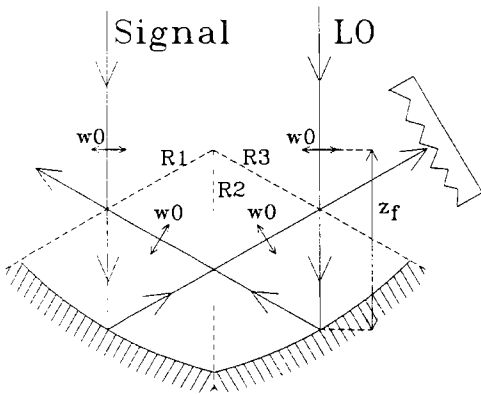


Figure 6: Configuration with 2 triangular FFPs in series. Transmission is calculated for $R1 = R3 = 0.243$ and $R2 = 0.664$.

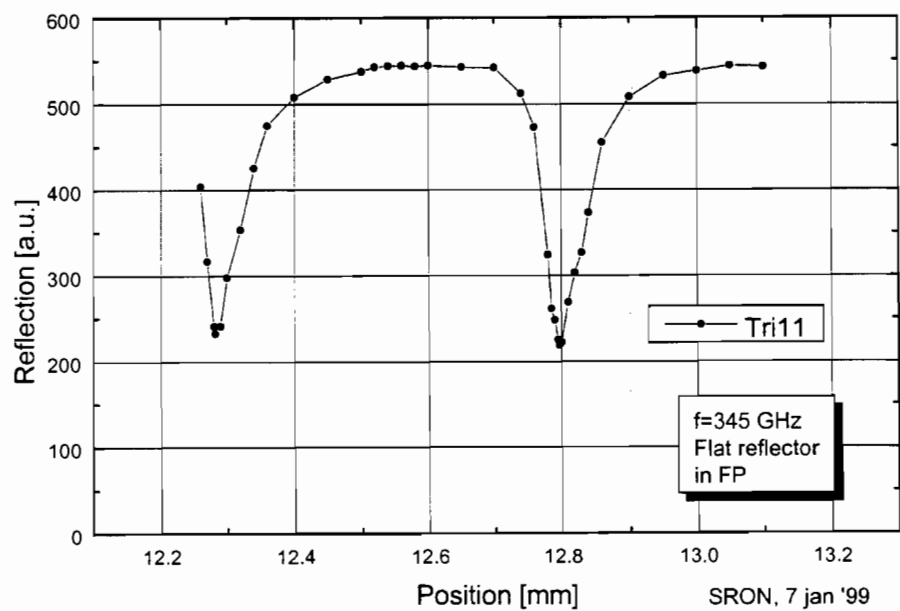
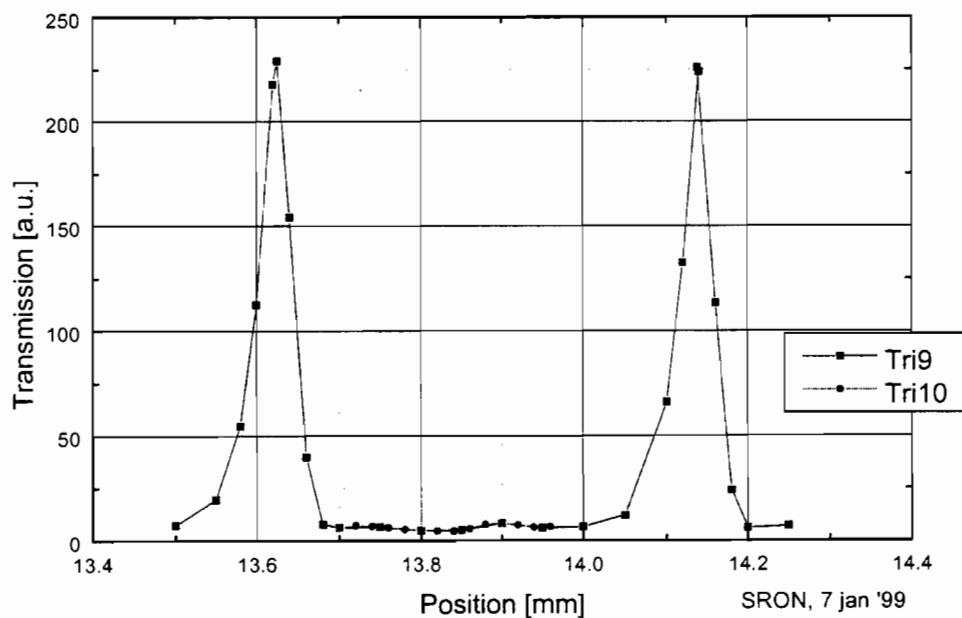


Figure 7: Transmission & reflection measured with prototype of triangular FFP at $f \cong 345$ GHz.